

Hubble Law from First Principles: Gravitational Friction as a Mechanism

C. Ortiz¹  and Raju S. Khatiwada² 

¹ Unidad Académica de Física, Universidad Autónoma de Zacatecas, Solidaridas, esq. la bufa S/N, Zacatecas , Zac , México, 98060.

²GoldenGate International College, Tribhuvan University, Kathmandu, 44600, Nepal.

E-mail: ortizgca@fisica.uaz.edu.mx

Abstract.

Hubble’s law, which relates the recessional velocities of galaxies to their distances, is traditionally explained through the Doppler redshift mechanism. In this letter, we propose an alternative interpretation by introducing Gravitational Friction (GF)—a process where photons lose energy through non-conservative, non-scattering interactions with the medium they traverse. By deriving Hubble’s law from first principles within the framework of energy conservation, we demonstrate how GF naturally produces the observed redshift, providing a deeper understanding of the underlying dynamics without relying solely on cosmic expansion. Furthermore, we outline feasible experiments to test and falsify the GF mechanism, offering a method to validate its role as a potential explanation for the observed redshift.

Introduction

Hubble’s law, first published in 1929 by Edwin Hubble in his seminal paper “A Relationship Between Distance and Radial Velocity among Extra-Galactic Nebulae” [1], established a linear relationship between the distances of galaxies and their recessional velocities. This significant discovery provided crucial evidence for the expanding Universe, fundamentally shaping the field of cosmology and establishing the basis of the standard model of cosmology.

Hubble’s law is an empirical relationship that links the observed radial velocity of a galaxy to its distance. It is important to note that the velocity of a galaxy is not measured directly; instead, it is inferred from the redshift of the galaxy’s spectral lines. This redshift is interpreted as a Doppler effect [2], which was the only recognized mechanism for explaining the redshift at the time of Hubble’s publication.

We must acknowledge that Hubble’s findings were grounded in the earlier work of Vesto M. Slipher, who was the first to measure the redshift of extragalactic objects using spectroscopy, identifying shifts in the spectral lines emitted by galaxies [3]. Although Slipher initially interpreted the redshift as a Doppler effect, he expressed

doubts about this interpretation but reported the observations as velocities because no alternative mechanisms were known at the time to explain the observed spectral shifts. Later, another mechanism, gravitational redshift, was theoretically proposed by Albert Einstein in 1908 and 1911 [4, 5] as a consequence of the equivalence principle, suggesting that the wavelength of light increases as it escapes a strong gravitational field. This mechanism was not experimentally verified until 1959 by Robert V. Pound and Glen A. Rebka [6].

A crucial development that significantly influenced the interpretation of Hubble's law came from Albert Einstein's 1915 general theory of relativity [7], which redefined gravity as the curvature of spacetime caused by mass and energy. This revolutionary framework allowed dynamic solutions for the structure of the Universe, breaking away from static models that had previously dominated scientific thought. In 1922, Alexander Friedmann provided one of the first solutions to Einstein's field equations, proposing a homogeneous and isotropic universe [8]. Friedmann's solutions predicted that the universe could expand, contract, or oscillate, depending on its matter content and initial conditions, radically challenging the notion of a static cosmos. In 1927, Georges Lemaître independently derived similar solutions and directly connected them to observational evidence, suggesting an expanding Universe as shown by the redshift of distant galaxies [9]. Lemaître's work not only introduced the idea of an evolving cosmos, but also offered the first estimates of the expansion rate, which would later become known as the Hubble constant. These theoretical insights, combined with Slipher's pioneering observations, played a crucial role in shaping the evolving understanding of the universe, significantly strengthening Hubble's interpretation of the redshift-distance relation and the concept of cosmic expansion.

The purpose of this paper is to redefine Hubble's law by introducing GF, a non-conservative mechanism rooted in the d'Alembert principle [10, 11], as a potential alternative to the traditional Doppler-based explanation for the redshift. We begin by thoroughly exploring the theoretical foundation of GF [12], followed by an estimation of the redshift it produces using the original data from Hubble's observations. Additionally, we propose feasible experimental setups designed to test and validate this mechanism, offering a framework to either confirm or challenge its contribution to the redshifts associated with cosmic expansion. Finally, we discuss the implications of our findings and how they might reshape our understanding of cosmic dynamics.

Gravitational Friction

Hubble's law traditionally relies on the Doppler effect to explain redshift, attributed the observed shift in the spectral lines emitted by stars to the relative motion of the source. However, this is not the only possible explanation. GF [12] presents an alternative mechanism, suggesting that the redshift could arise from interactions within a medium. This mechanism is grounded in the principle of virtual work, which states that the total virtual work of all forces in a system at equilibrium must equal zero. This approach

enables the application of d'Alembert's principle, which extends the concept of virtual work to dynamic systems by introducing inertial forces, allowing motion problems to be treated as if they were static.

In the scenario under consideration, a particle moves at constant velocity through a neutral, low-density medium. Since the velocity remains constant, the particle's kinetic energy does not change, and any energy loss is due to gravitational interactions with the medium. Using d'Alembert's principle, the forces acting on the particle are considered virtual displacements in a moving reference frame. This approach helps identify the effective forces along the trajectory of the particle. Due to the symmetry of the system, only forces perpendicular to displacement contribute.

The total work done by the particle on the medium is obtained by integrating these forces over the path of the particle. To apply this framework to photons, an effective mass is assigned in terms of wavelength / frequency [13]. Which leads to the following expression:

$$W = -\frac{1}{3} \frac{h f}{c^2} G \pi \bar{\rho} r^2. \quad (1)$$

In this equation, f represents the frequency of the photon, $\bar{\rho}$ is the average density along the path of the photon, and r is the distance traveled by the photon. The energy lost by the photon, expressed as the work done, is transferred to the medium as energy Q .

To further understand the implications of GF (1), we calculate the energy change experienced by the photon. For this analysis, we assume that the energy change is equivalent to what would occur in a moving reference frame, consistent with the principles of relative motion. This analogy allows us to integrate the energy dissipation effects into a dynamic framework, facilitating comparisons with observational data.

The initial energy of the photon is expressed as:

$$E_i = hf, \quad (2)$$

where h is Planck's constant and f is the photon's frequency. In a hypothetical moving reference frame, the photon's energy becomes:

$$E_f = \gamma hf = \frac{hf}{\sqrt{1 - \frac{v^2}{c^2}}}, \quad (3)$$

where γ is the Lorentz factor, and v represents the velocity of the source relative to the observer.

Applying the work-energy theorem, $\Delta E = -W + Q$, where W is the work done on the photon and Q is the energy dissipated in the medium. Assuming that $v \ll c$, we approximate the Lorentz factor for small velocities, resulting in the following expression for energy loss:

$$hf \frac{v^2}{c^2} = -W + Q. \quad (4)$$

The energy lost to the medium, represented by Q , is the result of the work W done by the medium through the GF mechanism. Since the only observable quantity is the

photon frequency shift[14], the energy transferred to the medium remains unaccounted for, that is, $Q = 0$. This leads to misinterpret it as an apparent velocity of the source.

$$v = \sqrt{\frac{2}{3}\pi G\bar{\rho}} \ r, \tag{5}$$

which can be related to the Doppler redshift, $z = \frac{v}{c}$, assuming $v \ll c$,

$$z = \left(\sqrt{\frac{2}{3c^2}\pi G\bar{\rho}} \right) r. \tag{6}$$

This relationship derived above is limited to the classical realm, including galactic, solar, and even terrestrial contexts. It is possible to derive the relativistic version of GF using the generalized redshift formula [14].

The relationship establishes a direct connection between the redshift, the average density of the medium, and the distance traveled by the photon, offering an alternative interpretation to the Doppler-based mechanism. The primary challenge lies in the accurate implementation of the formula for specific physical problems. In most cases, this requires precise modeling of the average density along the photon path to ensure the validity of the results.

Hubble's Law

The GF framework [12] offers an alternative interpretation of the redshift, challenging traditional attribution solely to the Doppler effect [2]. This model hypothesizes that the observed redshift arises not only from recessional velocities but also from cumulative interactions between photons and the medium they traverse, governed by density variations along the photon's path.

To accurately model the density, it is crucial to account for the overdensity present in the galactic neighborhood. For this, we employ a Gaussian density distribution that transitions smoothly to the cosmic mean density at larger scales, capturing both local and large-scale density variations.

Considering the observer's location within an overdense region of the Universe, the density profile is modeled as:

$$\bar{\rho} = \frac{\int_0^r [\rho_u + (\rho_g - \rho_u)e^{-\frac{x^2}{2\sigma^2}}] dx}{\int_0^r dx}, \tag{7}$$

where ρ_u represents the average cosmic density, ρ_g denotes the galactic density, and σ^2 is the variance of the Gaussian profile.

It is important to emphasize that the proposed density profile is a preliminary approximation for modeling the average density as observed from the Milky Way. This profile can be further refined to more accurately represent the conditions in the Earth neighborhood.

Using the formula of GF-derived redshift (6), the predicted redshift multiplied by the speed of light is expressed as:

$$zc = Hr = \sqrt{\frac{2}{3}\pi G \left[\rho_u + (\rho_g - \rho_u) \sqrt{\frac{\pi}{2}} \frac{\sigma}{r} \operatorname{erf} \left(\frac{r}{\sqrt{2}\sigma} \right) \right]} r. \quad (8)$$

which can be related to the Hubble “constant”, H . It becomes clear that the Hubble ‘constant’ is not truly constant; its value decreases with distance due to the influence of the Gaussian density profile. As measurements are made farther from the galaxy, its value gradually converges to a constant:

$$H = \sqrt{\frac{2}{3}\pi G \rho_u}. \quad (9)$$

GF provides a compelling explanation for Hubble’s law, incorporating the effects of density variations along the photon path. The model shows that the Hubble “constant” decreases with distance, gradually converging to a constant value determined by the cosmic mean density. The present interpretation defers from the traditional assumption of a constant Hubble law.

Constraining the model

In the following, we will constrain our model with observational data provided by the NASA/IPAC Extragalactic Database (NED).

The selected data set comprises 62 extragalactic objects extracted from the NED catalog [15, 16], chosen based on the following criteria: redshifts below 0.33 to minimize relativistic effects, measurements with established low uncertainty, and distances ranging from 50 Mpc to 1400 Mpc. Plus 18 Cepheid-calibrated distance SNe Ia, below 50 Mpc, reported by Riess et al. [17].

For the fitting process of the proposed model (8), one parameter is considered: the square root of the variance, σ with a flat prior in the range [0.1, 100]. The central density of the galaxy, $\rho_g = 3.413 \times 10^{-26} \text{ kg m}^{-3}$, is fixed to match the Hubble constant $H = 74.34 \text{ km s}^{-1} \text{ Mpc}^{-1}$ at late times. The density of the Universe, $\rho_u = 3.413 \times 10^{-26} \text{ kg m}^{-3}$, is also kept constant to ensure consistency with the Hubble constant at early times, $H = 64.34 \text{ km s}^{-1} \text{ Mpc}^{-1}$. It should be noted that this value of ρ_u is approximately four times the critical density predicted by the Λ CDM model.

We will quantify how well the model explains the observed data using the reduced Chi-square function χ_{red}^2 . Since the likelihood function is related to the merit function χ^2 through the relationship $\mathcal{L}(\Theta) \propto \exp[-\chi^2(\Theta)/2]$, it can also be expressed in terms of the reduced Chi-square function $\chi_{\text{red}}^2 = \chi^2/(N - p)$, where $N = 80$ is the number of data points and $p = 1$ is the number of free parameters of the model.

The merit function, which quantifies the discrepancy between the model predictions and the observed data, is given by:

$$\chi^2(\Theta) = \sum_{i=1}^N \left(\frac{V_{\text{obs}}^i - V_{\text{total}}(\Theta)}{\delta V_{\text{obs}}^i} \right)^2, \quad (10)$$

where $V_{\text{obs}}^i \pm \delta V_{\text{obs}}^i$ represents the 'observed velocity' ‡ and its associated uncertainty at the radial distance d_i .

The optimization procedure is conducted using the differential evolution algorithm provided by the SciPy library [18]. For the GF model, the reduced chi-square value is determined to be $\chi_{\text{red}}^2 = 8149.6$ with $\sigma = 25.63$. In the case of the classical Hubble law, two benchmark values for the Hubble constant are considered: $H_0 = 74.34 \text{ km s}^{-1} \text{ Mpc}^{-1}$, corresponding to the best estimate from late-time measurements [17], which yields $\chi_{\text{red}}^2 = 8,405.8$; and $H_0 = 64.34 \text{ km s}^{-1} \text{ Mpc}^{-1}$ representing the best estimate from early-time measurements [19], resulting in $\chi_{\text{red}}^2 = 22,058.7$. Figure 1 illustrates the results, providing a comparison between the constrained GF model (8) and the standard Hubble law.

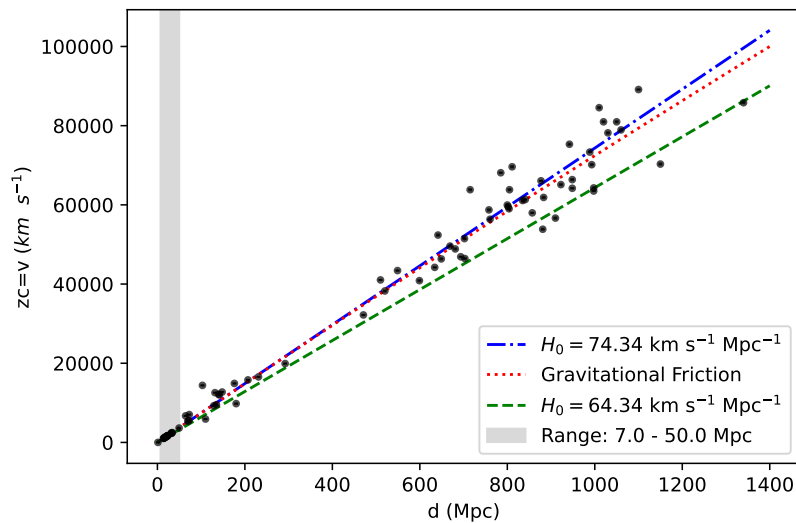


Figure 1. From top to bottom, Hubble's law with $H_0 = 73.24 \text{ km s}^{-1} \text{ Mpc}^{-1}$, GF model and Hubble's law $H_0 = 64.34 \text{ km s}^{-1} \text{ Mpc}^{-1}$. In gray area, Cepheids reported by Riess et al. [17].

From Fig. (2), we observe that the GF model aligns with the predicted values for late times, while Fig. (1) demonstrates how the model converges to the predicted value for early times. It is important to note that the values in the shaded region correspond to a purely classical regime, i.e., without contributions from either special or general relativity.

In the following section, we propose two experimental setups designed to test the GF mechanism. These experiments aim to directly assess the hypothesis by comparing theoretical predictions with empirical measurements, focusing on the potential role of medium interactions in photon energy loss.

‡ At cosmological distances, velocity can not be measured directly. The redshift is the measured quantity, and it is multiplied by the speed of light to express it as a recessional velocity.

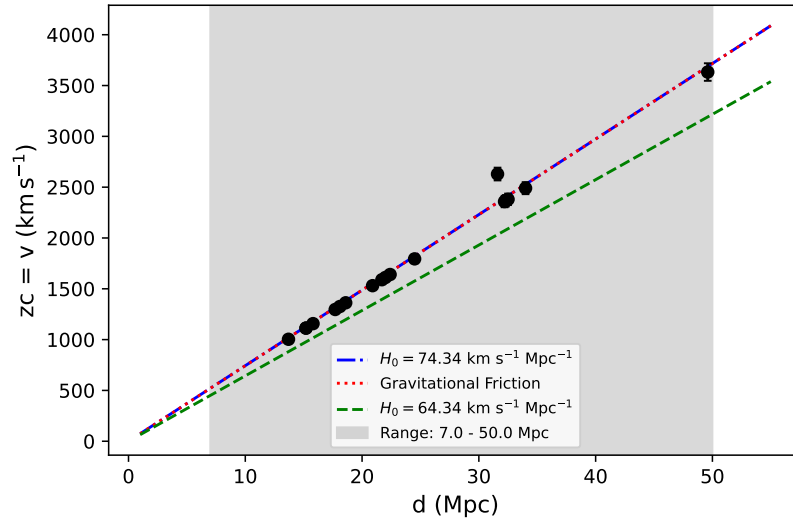


Figure 2. Sample of variable Cepheids reported by Riess et al. [17], with an average $H_0 = 73.24 \text{ km s}^{-1} \text{ Mpc}^{-1}$.

Falsifiability

A robust scientific hypothesis must be testable and falsifiable through experiment or observation. In this section, we propose two experimental setups to evaluate the GF model as an alternative explanation for the redshift. By comparing theoretical predictions with observational data, these experiments aim to assess whether GF can reliably explain the redshift-distance relationship.

The first experiment relies on instruments such as the Laser Interferometer Gravitational Wave Observatory (LIGO) [20], which employs laser interferometry to detect infinitesimal changes in the length of its arms. With a sensitivity capable of detecting distance variations as small as 10^{-19} m, approximately one-thousandth the diameter of a proton, LIGO provides an exceptionally controlled and precise environment. This makes it an ideal platform for testing the potential effects of GF on light.

GF depends on two variables: the distance traveled by the particle and the average density of the medium. The ultrahigh vacuum conditions of LIGO ensure minimal interference, with internal pressures ranging from 10^{-8} to 10^{-11} torr, achieved using advanced vacuum pumps to eliminate residual gases. According to the Advanced LIGO specifications [20], hydrogen is used as a residual gas within the system. Consequently, we have considered H_2 in our calculations to account for their contributions.

The Advanced LIGO Scientific Collaboration [20] reports a fixed arm cavity length of 3994.5 m (7989 m for a round trip) and a fixed wavelength of the emitted laser $\lambda_e = 1064$ nm. Using these parameters and the density of the medium, we calculate the change in photon energy and consequently the wavelength shift caused by GF.

The redshift z is related to the observational parameter λ by:

$$z = \frac{\lambda_o - \lambda_e}{\lambda_e}, \quad (11)$$

where λ_e is the emitted wavelength, and λ_o is the observed wavelength.

The change in wavelength $\Delta\lambda = \lambda_o - \lambda_e$ can be expressed as a function of the redshift,

$$\Delta\lambda = z\lambda_e. \quad (12)$$

Incorporating the GF redshift mechanism (8), the wavelength shift as a function of the density and distance becomes:

$$\Delta\lambda = \sqrt{\frac{2}{3c^2}\pi G\bar{\rho}r^2}\lambda_e. \quad (13)$$

Using LIGO's parameters, we estimate the predicted changes in wavelength across various density configurations. For this analysis, consider 10 different density values ranging from 10^{-7} to 10^{-16} kg m^{-3} , while maintaining a fixed photon path length of 8 km. These calculations provide insight into how the GF mechanism affects the wavelength shift across a range of realistic density scenarios.

Table 1. Predicted wavelength shifts $\Delta\lambda$ for various medium densities ρ .

Density (kg m^{-3})	Redshift z	$\Delta\lambda$ (m)
1.0×10^{-16}	3.1550×10^{-18}	3.3569×10^{-24}
1.0×10^{-15}	9.9770×10^{-18}	1.0615×10^{-23}
1.0×10^{-14}	3.1550×10^{-17}	3.3569×10^{-23}
1.0×10^{-13}	9.9770×10^{-17}	1.0615×10^{-22}
1.0×10^{-12}	3.1550×10^{-16}	3.3569×10^{-22}
1.0×10^{-11}	9.9770×10^{-16}	1.0615×10^{-21}
1.0×10^{-10}	3.1550×10^{-15}	3.3569×10^{-21}
1.0×10^{-09}	9.9770×10^{-15}	1.0615×10^{-20}
1.0×10^{-08}	3.1550×10^{-14}	3.3569×10^{-20}
1.0×10^{-07}	9.9770×10^{-14}	1.0615×10^{-19}

The results presented in Table (1) and the corresponding figure (3) illustrate the dependence of the wavelength shift $\Delta\lambda$ on the density of the medium ρ . As expected from the GF redshift mechanism, both the redshift z and the wavelength shift $\Delta\lambda$ increase with the density of the medium. These values fall well within the sensitivity range of modern interferometric detectors such as LIGO, demonstrating the feasibility of experimentally detecting these effects. However, it is crucial to emphasize that this estimate represents a lower bound on the expected gravitational redshift contribution, since external factors, including interactions with the experimental setup, could introduce variations and affect the calculations.

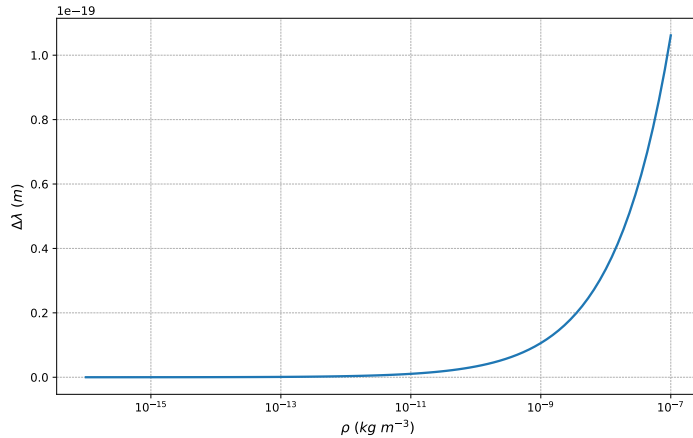


Figure 3. Expected wavelength shift $\Delta\lambda$ as a function of the decreasing density ρ .

The second experiment extends the testability of the redshift mechanism to a future space-based platform, such as the Laser Interferometer Space Antenna (LISA) [21]. Since LISA is not yet operational, this proposal represents a predictive test of the model, offering an opportunity to validate the GF mechanism once the platform becomes functional. Notably, the relative velocities of the satellites are determined based on redshift measurements, and the presence of a dissipative redshift mechanism, such as GF, could introduce systematic effects that impact the calibration process.

The European Space Agency (ESA) officially announced that the final configuration will adopt a distance of 2.5 million kilometers between each of the three satellites, with a fixed laser wavelength of $\lambda_e = 1064 \text{ nm}$ [22]. Considering the interplanetary density at 1 AU and the range of $\rho_{\text{IM}} = 1.2525 \times 10^{-20} \text{ kg m}^{-3}$ to $\rho_{\text{IM}} = 1.2525 \times 10^{-21} \text{ kg m}^{-3}$ [23], it is expected that the predicted redshift lies between 2.20493×10^{-19} and 2.20493×10^{-20} . As in LIGO's experiment, external factors, could introduce variations and affect the calculations.

Discussion

The results of this study demonstrate the efficacy of the (GF) model as an alternative explanation for Hubble's law. The GF model provides the best fit to the data, closely followed by the classical Hubble law with a fixed parameter $H_0 = 74.34 \text{ km s}^{-1} \text{ Mpc}^{-1}$.

It should be noted that, although the data used in this study correspond to late-time observations, the GF model converges toward the predicted value of the Hubble constant at early times, where traditional models face challenges in reconciling empirical measurements with theoretical predictions.

The GF mechanism complements existing redshift mechanisms, such as the Doppler effect and gravitational redshift, rather than discarding them. Observed redshifts result from multiple mechanisms, each contributing on the basis of the astrophysical and

cosmological context.

Conclusion

This work explores the GF redshift as an alternative explanation for the redshift-distance relationship traditionally attributed to the Doppler effect within Hubble's law. We must acknowledge that the GF redshift mechanism is derived from first principles, based on the principle of virtual work and d'Alembert's principle. This provides fundamental insights into the nature of this phenomenon, as opposed to the empirical nature of Hubble's law. By deriving the redshift formula from the first principles and incorporating density-dependent interactions along the photon path, the GF model offers a novel perspective on cosmic dynamics.

Our theoretical predictions indicate that the Hubble parameter is not constant but decreases as the density decreases, eventually converging to a value determined by the cosmic mean density.

The GF mechanism not only aligns with observed redshift trends, but also opens the door to further experimental validation and refinement. It is important to note that the present model is classical, relying on principles of mechanics and neglecting relativistic effects. We are currently extending the implementation of non-conservative mechanisms to the general relativity framework, and such work will be published elsewhere.

The experimental feasibility of this model is supported by a highly controlled environment like LIGO's, which provides the precision necessary to detect the predicted wavelength shifts under varying medium densities. The calculations presented confirm that the effects of GF are both observable and measurable within current technological capabilities. This framework also highlights the importance of considering alternative redshift mechanisms in precision experiments, such as LIGO and LISA, where even subtle effects can influence results and calibration processes.

Acknowledgments

C.O. would like to acknowledge Daniel O. for his critical feedback.

References

- [1] Hubble E 1929 *Proc. Nat. Acad. Sci.* **15** 168–173
- [2] Doppler C 1842 *Abhandlungen der Königlichen Böhmischen Gesellschaft der Wissenschaften*
- [3] Slipher V M 1913 *Lowell Observatory Bulletin* **2** 56–57
- [4] Einstein A 1908 *Jahrbuch der Radioaktivität und Elektronik* **4** 411–462
- [5] Einstein A 1911 *Annalen der Physik* **340** 898–908
- [6] Pound R V and Rebka G A 1959 *Phys. Rev. Lett.* **3**(9) 439–441
- [7] Einstein A 1915 *Sitzungsberichte der Königlich Preussischen Akademie der Wissenschaften* 844–847
- [8] Friedmann A 1922 *Zeitschrift für Physik* **10** 377–386
- [9] Lemaitre G 1927 *Annales Soc. Sci. Bruxelles A* **47** 49–59

- [10] Gantmacher F 1970 *Lectures in Analytical Mechanics* (Moscow: Mir Publishers) translated from the Russian edition published in 1966
- [11] Lanczos C 1986 *The Variational Principles of Mechanics* 4th ed Dover Books on Physics (New York: Dover Publications) ISBN 9780486650678 originally published in 1949 by the University of Toronto Press
- [12] Ortiz C and Khatiwada R S 2023 *Scientific Reports* **13** 10364 URL <https://doi.org/10.1038/s41598-023-36977-6>
- [13] Tu L C, Luo J and Gillies G T 2004 *Reports on Progress in Physics* **68** 77 URL <https://dx.doi.org/10.1088/0034-4885/68/1/R02>
- [14] Ortiz C and Ibarra-Castor F 2024 *Scientific Reports* **14** 22638 URL <https://doi.org/10.1038/s41598-024-73191-4>
- [15] NASA/IPAC E 2023 *NED Extragalactic Database (NED)* Accessed: 2024-12-04 URL <https://ned.ipac.caltech.edu/>
- [16] Cook D O, Mazzarella J M, Helou G, Alcalá A, Chen T X, Ebert R, Frayer C, Kim J, Lo T, Madore B F, Ogle P M, Schmitz M, Singer L P, Terek S, Valladon J and Wu X 2023 *apjs* **268** 14 (*Preprint* 2306.06271)
- [17] Riess A G, Macri L M, Hoffmann S L, Scolnic D, Casertano S, Filippenko A V, Tucker B E, Reid M J, Jones D O, Silverman J M, Chornock R, Challis P, Yuan W, Brown P J and Foley R J 2016 *apj* **826** 56 (*Preprint* 1604.01424)
- [18] Virtanen P *et al.* 2020 *Nature Methods* **17** 261–272
- [19] Collaboration P, Aghanim N *et al.* 2020 *Astronomy & Astrophysics* **641** A6
- [20] Aasi J *et al.* 2015 *Classical and Quantum Gravity* **32** 074001
- [21] Amaro-Seoane P, Audley H, Babak S, Baker J, Barausse E, Bender P, Berti E, Binetruy P, Born M, Bortoluzzi D, Camp J, Caprini C, Cardoso V, Colpi M, Conklin J, Cornish N, Cutler C, Danzmann K, Dolesi R, Ferraioli L, Ferroni V, Fitzsimons E, Gair J, Gesa Bote L, Giardini D, Gibert F, Grimani C, Hallain H, Heinzel G, Hertog T, Hewitson M, Holley-Bockelmann K, Hollington D, Hueller M, Inchauspe H, Jetzer P, Karnesis N, Killow C, Klein A, Klipstein B, Korsakova N, Larson S L, Livas J, Lloro I, Man N, Mance D, Martino J, Mateos I, McKenzie K, McWilliams S T, Miller C, Mueller G, Nardini G, Nelemans G, Nofrarias M, Petiteau A, Pivato P, Plagnol E, Porter E, Reiche J, Robertson D, Robertson N, Rossi E, Russano G, Schutz B, Sesana A, Shoemaker D, Slutsky J, Sopuerta C F, Sumner T, Tamanini N, Thorpe I, Troebs M, Vallisneri M, Vecchio A, Vetrugno D, Vitale S, Volonteri M, Wanner G, Ward H, Wass P, Weber W, Ziemer J and Zweifel P 2017 *arXiv e-prints* arXiv:1702.00786
- [22] Colpi M *et al.* 2024 (*Preprint* 2402.07571)
- [23] Mann I, Czechowski A and Meyer-Vernet N 2010 Dust in the interplanetary medium—interactions with the solar wind *AIP Conference Proceedings* vol 1216 (American Institute of Physics) pp 491–496